

# Development of a Fiber-Coupled Dispersion Interferometer for Low Electron Density Measurements

N. R. Hines<sup>1</sup>, Sonal Patel<sup>2</sup>, Daniel J Scoglietti<sup>2</sup>, Mark A Gilmore<sup>1</sup>, S. L. Billingsley<sup>1</sup>, R. H. Dwyer<sup>1</sup>, Thomas Awe<sup>2</sup>, Darrell Armstrong<sup>2</sup>, David Bliss<sup>2</sup>, George Laity<sup>2</sup>, Michael E Cuneo<sup>2</sup>

1) The University of New Mexico, Albuquerque, NM 2) Sandia National Laboratories, Albuquerque, NM

\*Supported by the Laboratory Directed Research and Development program at Sandia National Laboratories, a multimission laboratory managed and operated by National Technology and Engineering Solutions of Sandia LLC, a wholly owned subsidiary of Honeywell International Inc. for the U.S. Department of Energy's National Nuclear Security Administration under contract DE-NA0003525. This project was supported by LDRD project number 222428. SAND Number: SAND2022-6339 C

## Objective

- Development of a fiber-based Dispersion Interferometer (DI) will enable the first direct measurements of electron sheath flow on Z, between  $10^{14} - 10^{18} \text{ elec/cm}^2$ .
  - Reduce the present lower limit of the available electrode plasma density measurements by a factor of 100.
  - Perform studies on reliable delivery of current to magnetically driven loads, which can influence electrode plasmas and reduce coupling efficiency.
    - Plasma is spawned via ohmic heating of the electrode; a sheath is formed due to the surface charge generated as ions and electrons diffuse from the plasma at different rates.
- This DI design operates with a Fundamental (F) wavelength at 1550 nm, CW 0.65 Watts, with frequency-doubling to a Second-Harmonic (SH) wavelength at 775 nm.
  - The design is fiber-coupled due to spatial limitations inside Magnetically Insulated Transmission Lines (MITLs).

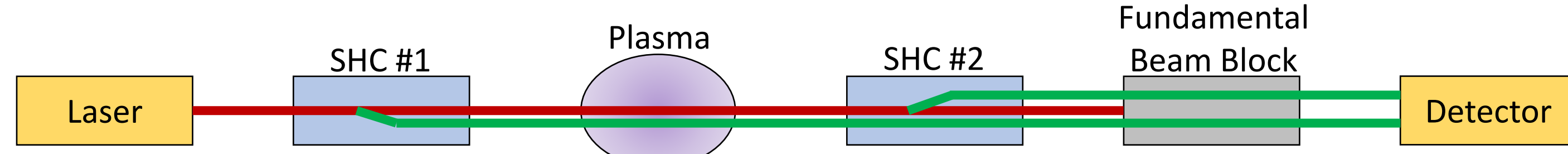


**FIG 1:** Diagram of basic DI design composed of the laser source, the first second-harmonic crystal (SHC), the plasma itself, the second second-harmonic crystal, a fundamental beam block, and a detector.

- First, the diagnostic has been installed on the UNM Helicon-Cathode (HelCat) plasma device<sup>1</sup>.
  - Comparisons against line-average electron density measurements made via a 94 GHz mm-wave interferometer verify the DI's lower bound accuracy.
- Second, it will be deployed at Sandia's Mykonos 1-MA driver.
- Third, it will be fielded on Sandia's Z machine.
  - Measurements will be made of electron sheath flow on MITLs.

## UNM HelCat Experimental Setup

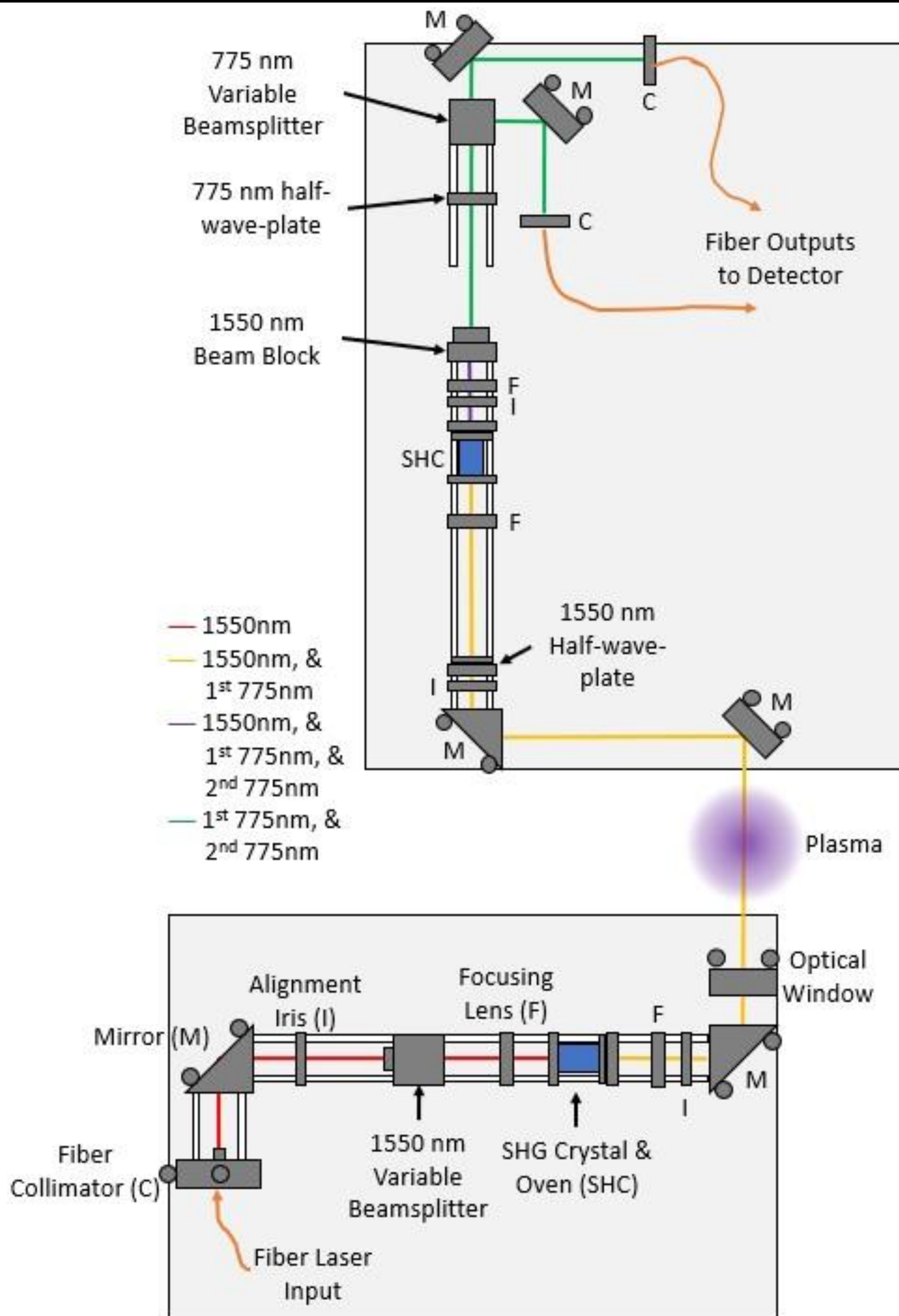


**FIG 2.1:** A 2-D horizontal-plane diagram of the DI optical setup on UNM's HelCat device.

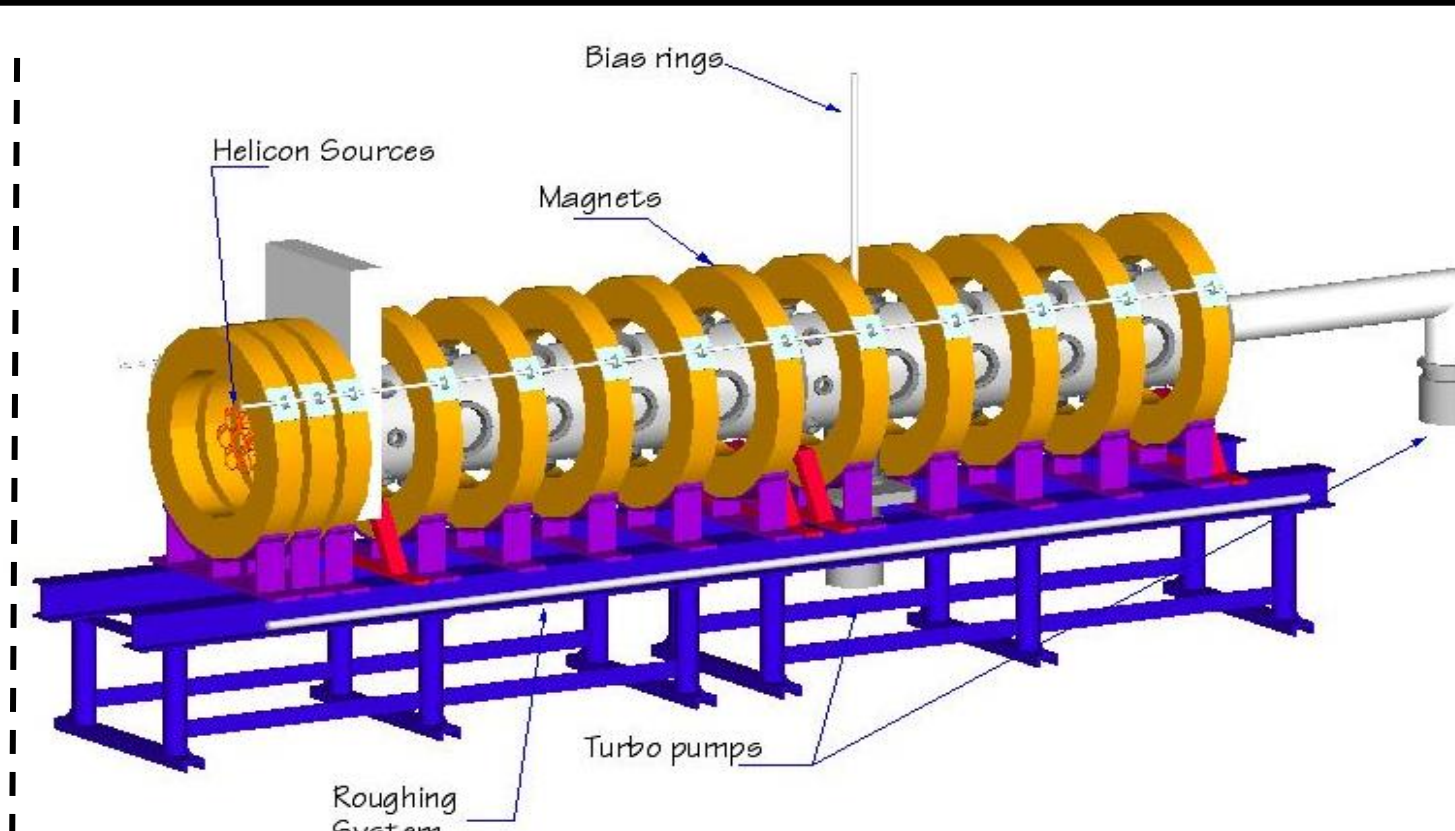
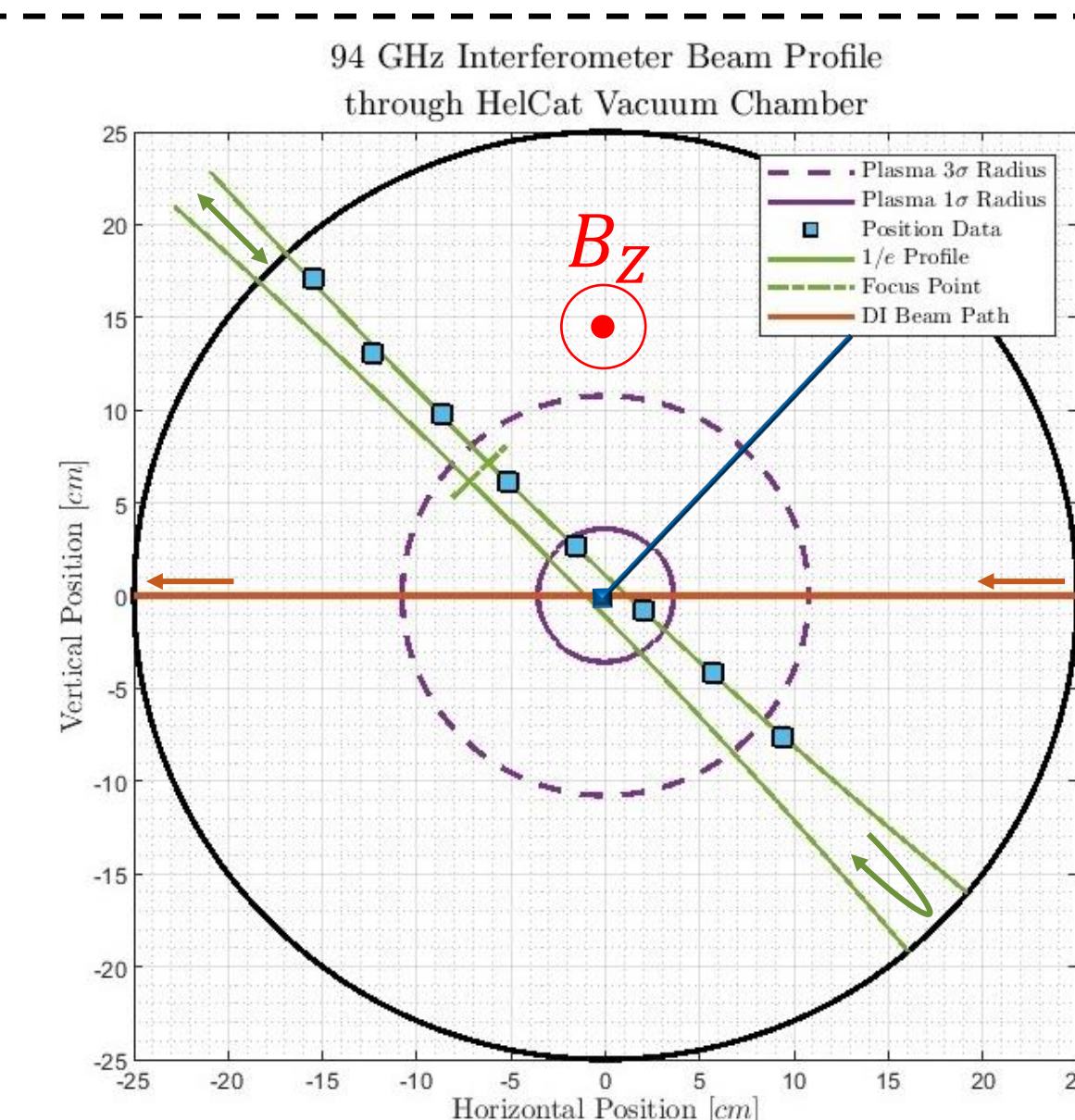


**FIG 2.2:** A 3-D render of UNM's HelCat device.



- (red) The DI path, traveling through plasma once.
- (blue) Radially scanning double Langmuir probe.
- (green) The 94 GHz mm-wave interferometer path, traveling through plasma twice.

**FIG 2.3:** A 2-D axial cross section diagram of the three electron density diagnostics on UNM's HelCat device.

## DI Data

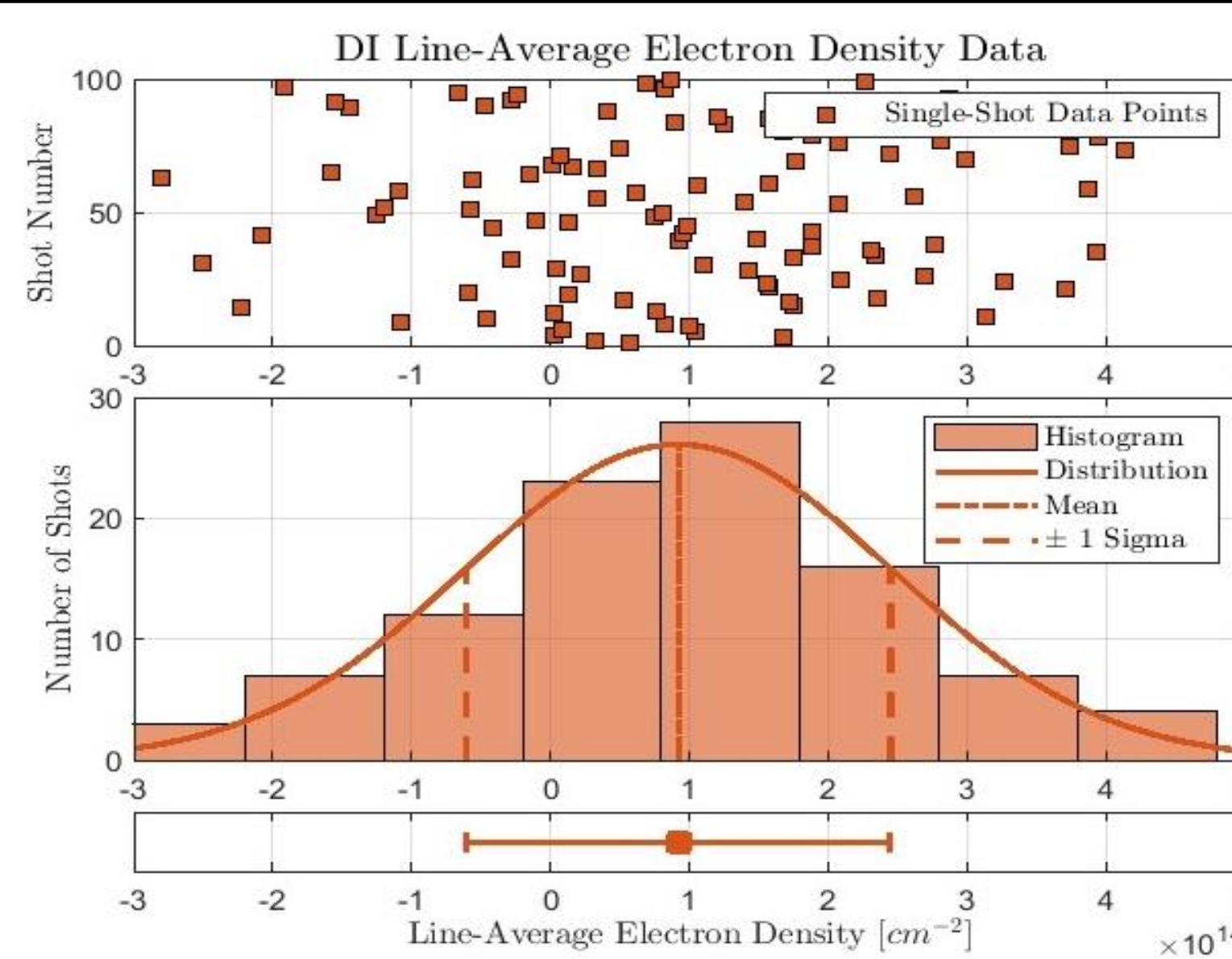


**FIG 3.1:** DI 100 shot line-averaged electron density measurements made on the UNM HelCat device, and a normalized representation.

- The DI is measuring a median line-averaged electron density of  $9.23 \times 10^{13} \text{ elec/cm}^2 \pm 15.27 \times 10^{13} \text{ elec/cm}^2$ .
  - The spread is mostly caused by the large system drift ( $170 \text{ mV} \pm 29 \text{ mV}$ , over 20 seconds) and system noise ( $\pm 20 \text{ mV}$ ). Expected signals from the HelCat plasma are  $\sim 5 \text{ mV}$ .

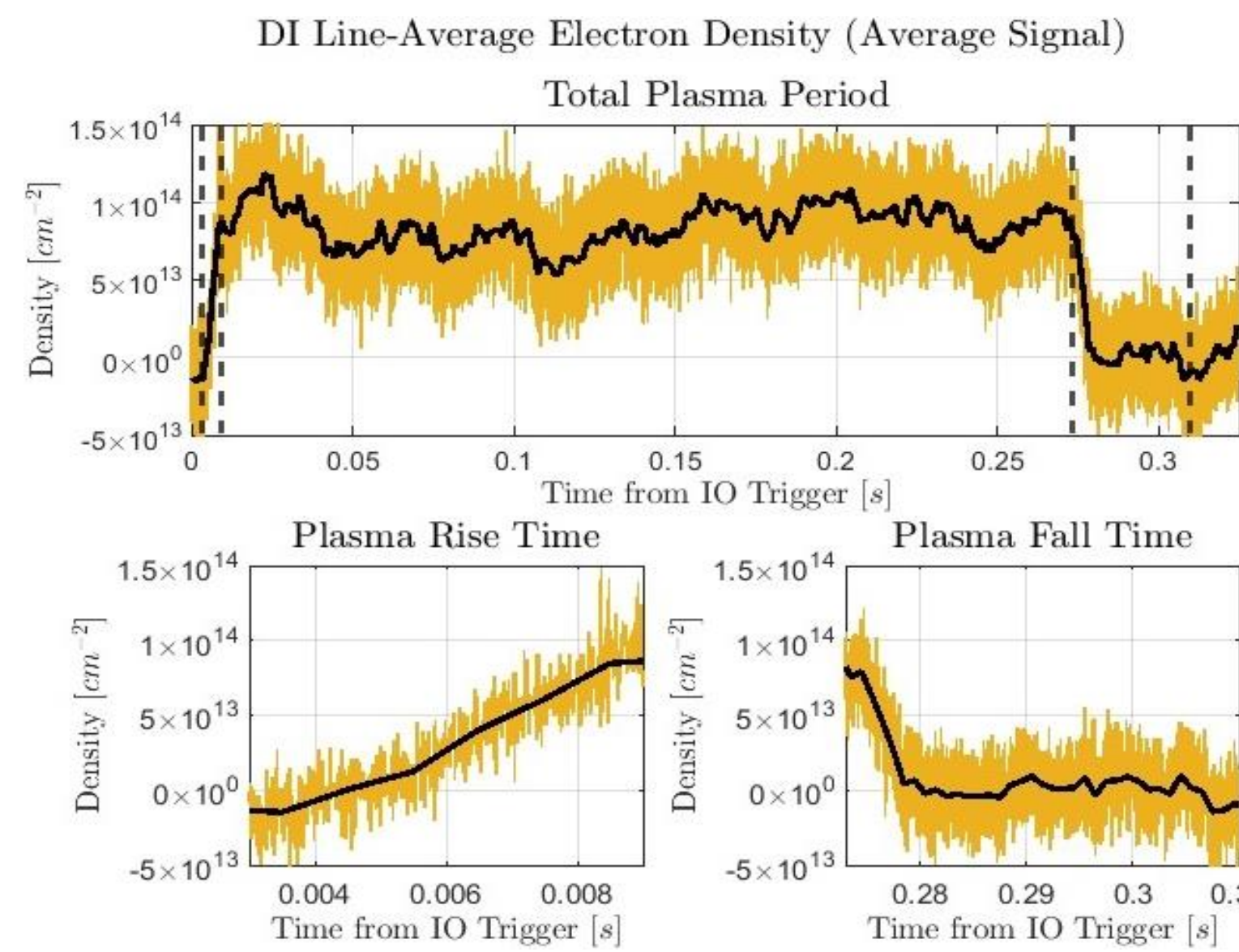


**FIG 3.2:** DI 100 shots' averaged signal (reduced noise and drift) density data taken on the UNM HelCat device (yellow) and noise filtered (black).

## 94 GHz Interferometer Data

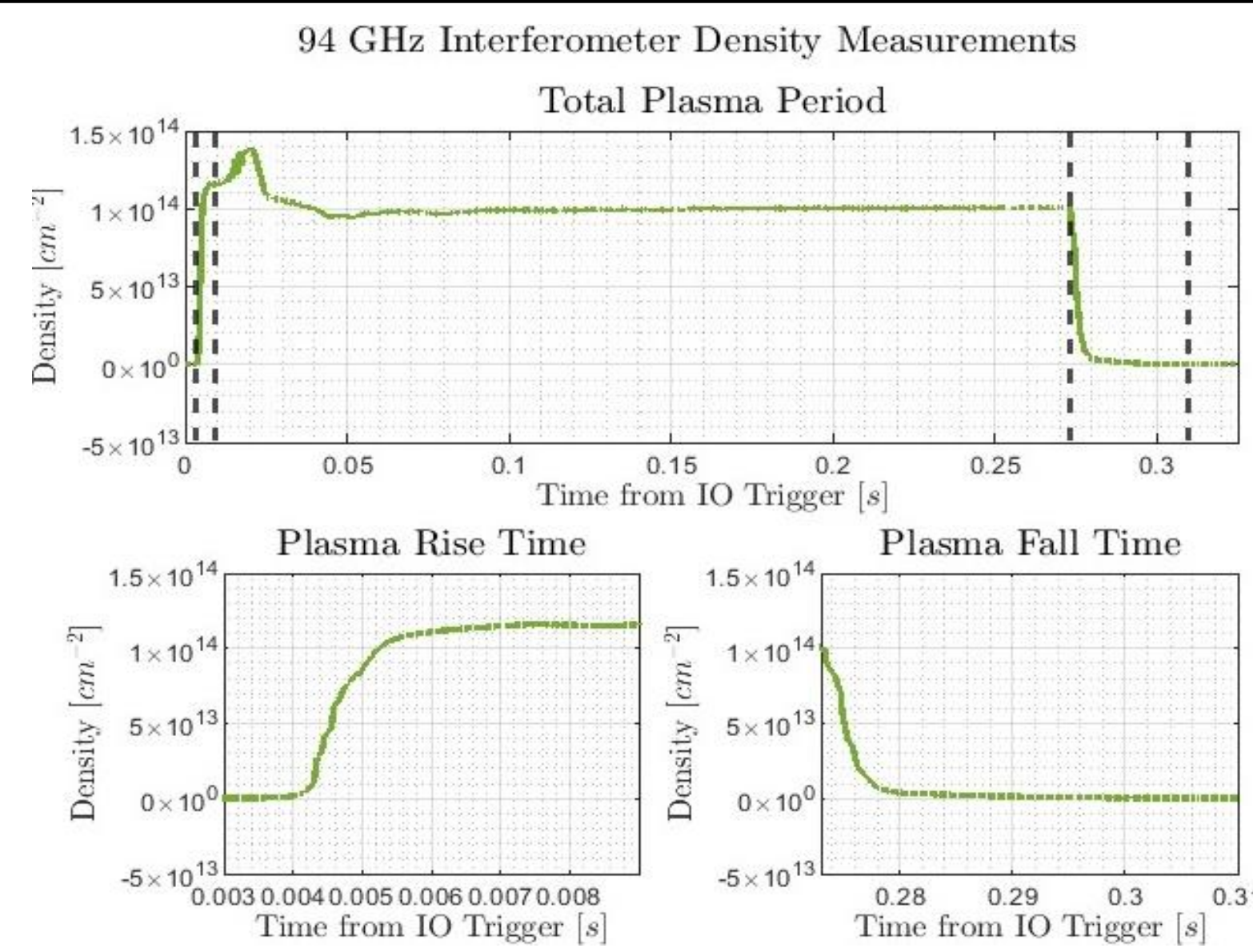


**FIG 4.1:** 94 GHz interferometer average density data from 10 shots on the UNM HelCat device. This measured a line-averaged electron density of  $10.13 \times 10^{13} \text{ elec/cm}^2 \pm 4.79 \times 10^{11} \text{ elec/cm}^2$ .

## HelCat Electron Density Results

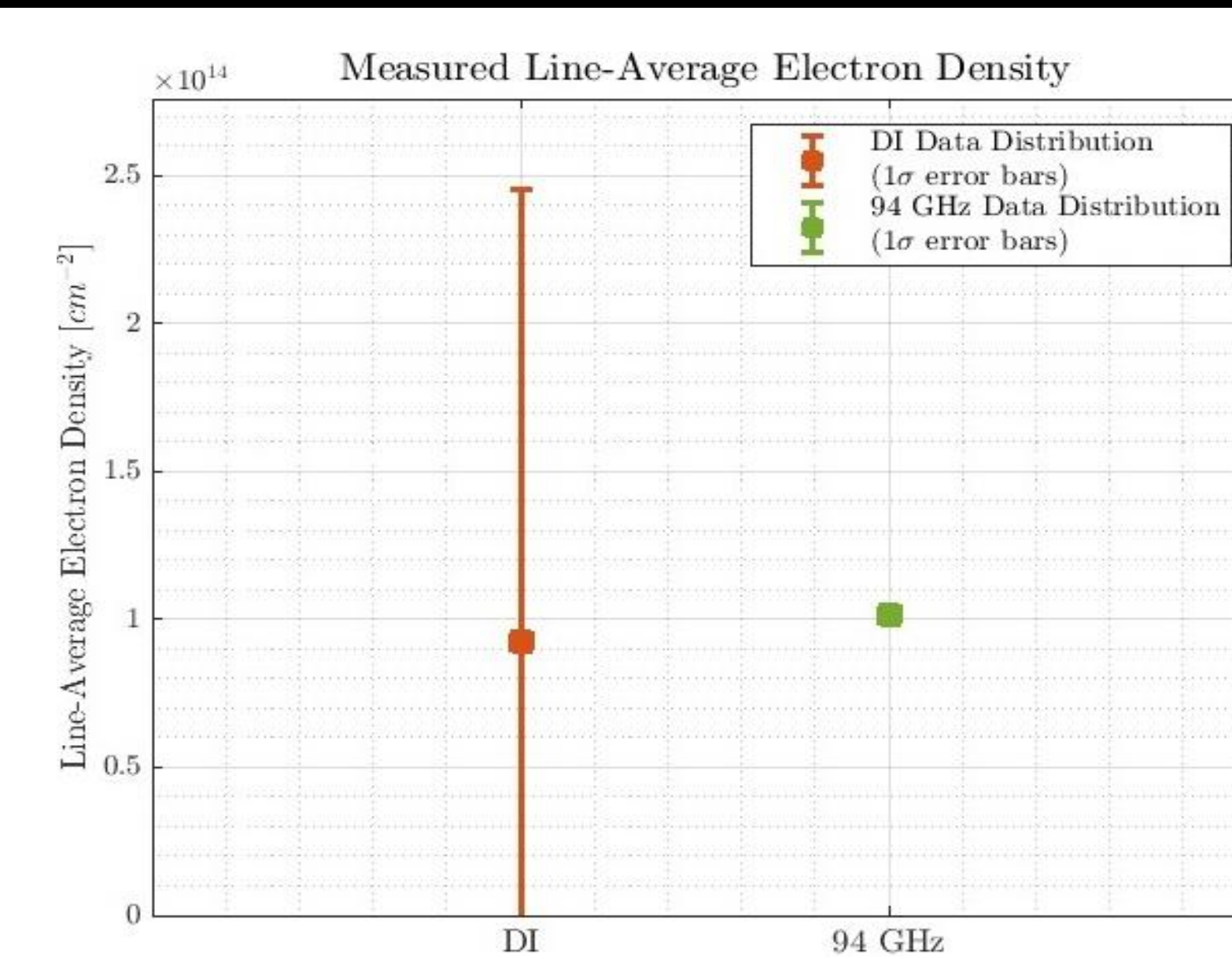


**FIG 6.1:** The measured line-averaged electron density from the laser DI data distribution, and the 94 GHz interferometer data distribution.

## Double Langmuir Probe Data

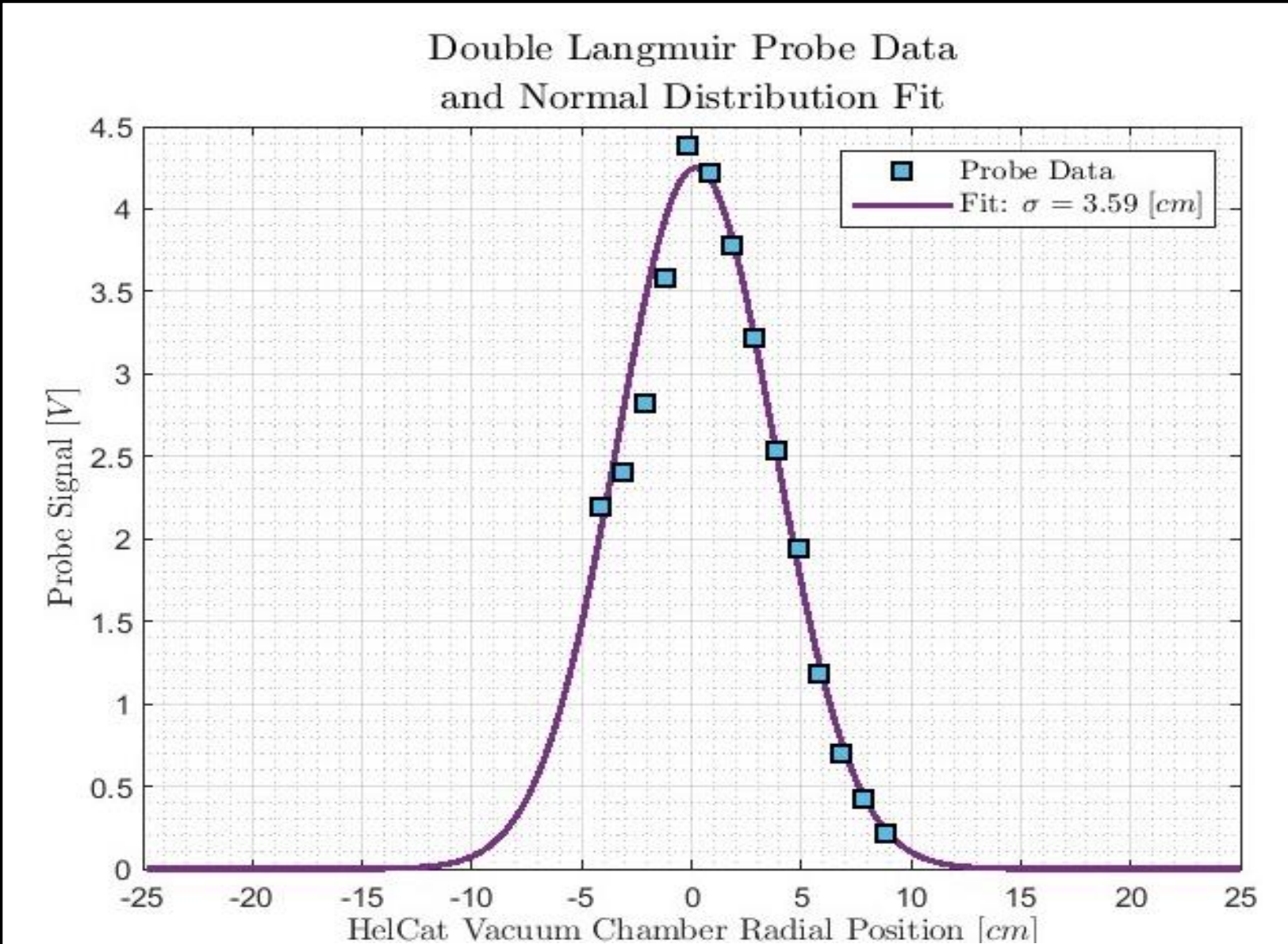


**FIG 5.1:** Double Langmuir probe radial sweep data and normalized distribution curve fit. The double Langmuir probe matches closely with a normalized distribution with  $\sigma = 3.59 \text{ cm}$ .

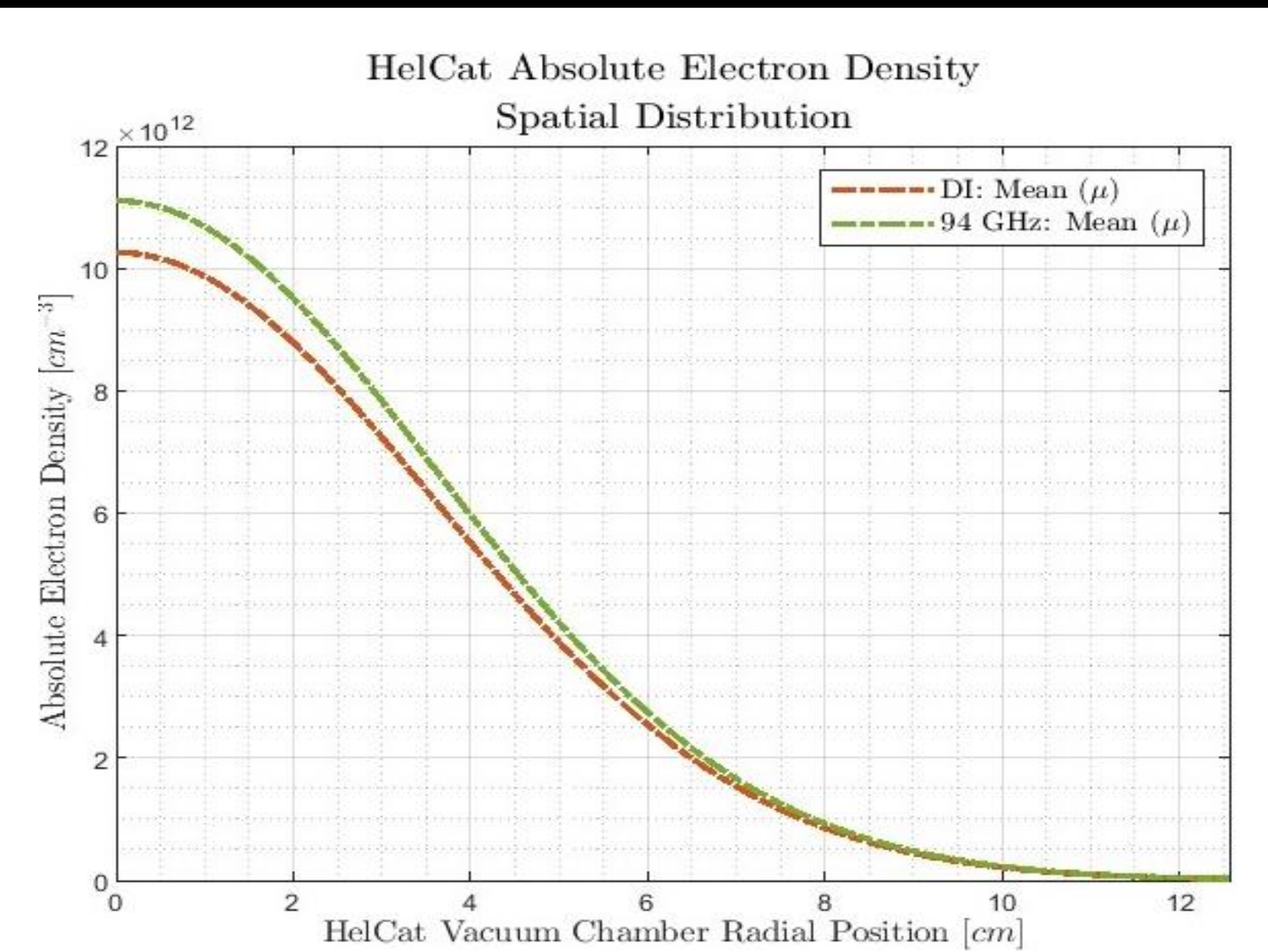


**FIG 6.2:** Absolute electron density distribution in the UNM HelCat chamber plot corresponding to the line-averaged electron density data collected in FIG. 6.1 and the spatial distribution data collected in FIG. 5.1.

## Principles of Operation

- The DI system is effectively measuring the relative phase changes that two wavelength undergo whilst passing through a magnetized plasma in x-mode (the electric field of the laser beam is perpendicular to the background magnetic field), via a wavelength dependent index of refraction,  $N_x$ :
 
$$N_x = \sqrt{1 - \left( \frac{n_e e^2 \lambda^2}{\epsilon_0 m_e 4\pi^2 c^2} \right) \left( \frac{4\pi^2 c^2 - n_e e^2}{\lambda^2 - \epsilon_0 m_e} \right)} \quad (1)$$
- The total phase change undergone from vacuum to plasma is related to the two wavelengths,  $\lambda_F$  and  $\lambda_{SH}$ , along the plasma path length,  $l$ , background magnetic field,  $B$ , and electron density,  $n_e$ , as:
 
$$\Delta\phi_{total} = \left( 2 * \frac{2\pi}{\lambda_F} \int_0^l \left( 1 - \sqrt{1 - \left( \frac{n_e e^2 \lambda_F^2}{\epsilon_0 m_e 4\pi^2 c^2} \right) \left( \frac{4\pi^2 c^2 - n_e e^2}{\lambda_F^2 - \epsilon_0 m_e} \right)} \right) \right) - \left( \frac{2\pi}{\lambda_{SH}} \int_0^l \left( 1 - \sqrt{1 - \left( \frac{n_e e^2 \lambda_{SH}^2}{\epsilon_0 m_e 4\pi^2 c^2} \right) \left( \frac{4\pi^2 c^2 - n_e e^2}{\lambda_{SH}^2 - \epsilon_0 m_e} \right)} \right) \right) \quad (2)$$
- Use the measured voltage signals to calculate the effective total change in radians,  $\Delta\phi_{total}$ .
- Use a numerical solver to iteratively calculate the average electron density,  $n_e$ , from equation (2).
- Multiply by the total plasma path length,  $l$ , to calculate the line-average electron density,  $\bar{n}_e$ .
  - For the HelCat system:  $\bar{n}_e \approx 10e13 [\text{electrons per cm}^2]$
- For absolute electron density calculations, use independent probe data to find the normalized electron density profile as a function of position,  $p_e(x)$ .
- Replace the average electron density factor,  $n_e$ , with the absolute density profile,  $p_e(x)n_{e,max}$ .
  - For the HelCat system:  $n_{e,max} \approx 1e13 [\text{electrons per cm}^3]$

## Future Work

- Reduce Noise and Drift
  - Better SHC insulation and temp. control, DAQ, and shorter plasma periods of pulsed devices).
- Move the diagnostic to Sandia National Labs' Mykonos and Z pulsed power machines.
- Develop a multi-channel DI design for spatial resolution capabilities.

## References

- Lynn AG, "The HelCat dual-source plasma device," Rev Sci Instrum. Vol. 80, pp. 103501, 2009
- Fernando Brandi and Francesco Giammarco, "Harmonic interferometry in the visible and UV, based on second- and third-harmonic generation of a 25 ps mode-locked Nd:YAG laser," Opt. Lett. 33, 2071-2073, 2008.
- V. Licht, "A sensitive dispersion interferometer with high temporal resolution for electron density measurements," Rev Sci Instrum. vol. 71, no. 7, pp. 2710-2715, 2000.
- M. A. Van Zeeland, "Fiber optic two-color vibration compensated interferometer for plasma density Measurements," Rev Sci Instrum. vol. 77, pp. 10F325, 2006.